International Journal of Nanoelectronics and Materials
IJNeaM
ISSN 1985-5761 | E-ISSN 2232-1535

Hexagonal Enhanced Porous GaN with Delayed Integrated Pulse Electrochemical (iPEC) Etching

Nurul Syuhadah Mohd Razali[a], Alhan Farhanah Abd Rahim[a,*], Nur Sabrina Mohd Hassan[a], Rosfariza Radzali[a], Ainorkhilah Mahmood[b], Syarifah Norfaezah Sabki[c,d], Irni Hamiza Hamzah[a], Mohaiyedin Idris[a] and Mohamed Fauzi Packeer Mohamed[e]

[a]*Electrical Engineering Studies, College of Engineering, Universiti Teknologi MARA, Cawangan Pulau Pinang, 13500 Permatang Pauh, Pulau Pinang, Malaysia*
[b]*Department of Applied Science, Universiti Teknologi MARA, Cawangan Pulau Pinang, 13500 Permatang Pauh, Pulau Pinang, Malaysia*
[c]*Faculty of Electronic Engineering Technology, Universiti Malaysia Perlis (UniMAP), 02600 Arau, Perlis, Malaysia*
[d]*Center of Excellence (COE) Microsystem Technology, Universiti Malaysia Perlis (UniMAP), 02600 Arau, Perlis, Malaysia*
[e]*School of Electrical and Electronic Engineering, Engineering Campus, Universiti Sains Malaysia, 14300 Nibong Tebal, Pulau Pinang, Malaysia*
** Corresponding author. Tel.: +019-265 2180; e-mail: alhan570@uitm.edu.my*

Received 19 February 2024, Revised 15 March 2024, Accepted 23 April 2024

ABSTRACT

This present study investigates the effect of time delay (T_d) on the formation of porous GaN (P-GaN) using integrated pulse electrochemical (iPEC) etching. Porous GaN (P-GaN) was formed by etching an N-type GaN wafer with a 4% KOH electrolyte for 60 minutes under an ultraviolet (UV) lamp at a current density of 80 mA/cm^2. A T_d of 120 minutes was applied before electrochemically etching the P-GaN sample. The top view image of the field emission scanning electron microscopy (FESEM) revealed a significant difference when a T_d was applied. A dense and uniform hexagonal P-GaN was obtained from the T_d iPEC sample, while the non-T_d sample exhibited a multi-layered hexagonal porous structure with unfinished pore-etched areas. Higher porosity and deeper pores were observed in the T_d sample. Intense high-resolution X-ray diffraction (HR-XRD) peak intensity was observed in the T_d iPEC sample with a lower full width half maximum (FWHM), indicating that the sample had better crystallinity. The Raman spectra of the sample anodized with a T_d exhibited higher Raman peak intensity and a slight shift to a higher frequency concerning as-grown GaN, indicating better crystallinity and a tensile stress relaxation of 0.24 GPa. Post etching, a blue shift of the photoluminescence (PL) peak, from 364 nm (as-grown GaN) to 363 nm (P-GaN), was observed, and a small PL peak started to form around 385 nm compared to the as-grown GaN due to the relaxation of the tensile stress, which modified the bandgap. The PL peak intensity of the Td sample was higher than the non-Td sample, indicating that the porosity and uniformity allowed more light interaction with the material, resulting in more efficient photon absorption and emission. The results indicated that potentially efficient optoelectronics devices can be fabricated on a P-GaN using a combination of electroless and electrochemical etching of the GaN epitaxial layer.

Keywords: *Porous Structure, Porous GaN, Pulse Electrochemical Etching, Surface Morphology, Time Delay*

1. INTRODUCTION

Optoelectronic devices are electronic devices that operate on either electrically driven light sources, such as laser diodes and light-emitting diodes (LED), or by converting light to an electrical current, such as photovoltaic (PV) cells that can govern the light propagation [1]. These semiconductor optoelectronic devices are important in communications and information technology [2]. Industry demand is leading both fields to grow immensely, and there is a need to enhance optoelectronic performance.

Over the past few decades, silicon (Si)-based devices have advanced and paved the way in the semiconductor industry due to inexpensive materials and availability in large sizes. However, researchers claim that Si is unstable for optoelectronic applications due to its indirect bandgap, which may reduce its efficiency as a light emitter [3]. This phenomenon leads to inadequate operation of optoelectronic devices.

There are various ways of enhancing the performance of optoelectronic devices. One way is to apply porous structures to the semiconductor material [4–7]. The porous structures of semiconductors is a subject of interest as their physical and chemical properties are unique in that they differ from those of bulk materials [4,6,8,9]. Through the use of these structures, the quantum confinement effect is predicted to increase the density of electrons, phonons, and carriers of electron-hole pair recombination. Researchers have recently used this porous structure to improve the performance of optoelectronic devices as it provides a high surface area, a band gap shift, and efficient luminescence properties [3,6].

Porous structures grown on III-nitride compound materials have gained a lot of attention because of their assured potential for optoelectronic devices and conduction in the blue and UV regions of the light

spectrum. Porous gallium nitride (P-GaN) has been examined due to its large direct band gap and thermal, mechanical, and chemical stability [6,10,11]. The physical characteristics of gallium nitride (GaN) allow the creation of a structure in a harsh environment; hence, the creation of a P-GaN structure was intended [12].

GaN has emerged as a significant material in optoelectronics due to its unique properties and wide-ranging applications. GaN, an III-V semiconductor, exhibits exceptional electronic and optical characteristics, including a wide bandgap, high electron mobility, and efficient light emission spanning the visible and UV spectrum [13,14]. These attributes make GaN highly desirable for applications such as solid-state lighting, power electronics, and high-frequency (HF) devices. However, as the full potential of GaN-based devices is yet to be realised, researchers continue to explore innovative strategies to improve their performance.

Although GaN offers numerous advantages, it also presents certain limitations. One challenge is the realisation of efficient light extraction from GaN-based devices. The high refractive index of GaN causes total internal reflection at the semiconductor-air interface, hindering the efficient emission of light. Additionally, non-radiative recombination processes in GaN can lead to the loss of energy as heat rather than light [13,15]. These limitations have prompted investigations into alternative approaches to enhancing the optical properties of GaN.

A suitable fabrication technique is required to produce a uniformly porous surface on semiconductor materials. Conventionally, a porous structure on a semiconductor surface is created using direct current photo-assisted electrochemical (DCPEC) etching [16–19]. However, this etching method necessitates complex and careful parameter control to achieve uniform porosity and typically produces a non-uniform porous structure that can cause low light extraction efficiency in optoelectronic devices. Furthermore, the hydrogen (H_2) bubbles that form in the pores significantly delay the etching process. As a result, the iPEC etching was necessary because it allows the sample to rest by temporarily pausing the current. This enables the sample to eject the H2 bubbles while simultaneously allowing fresh HF to penetrate the pores and react with the substrate, which can significantly enhance the etching process.
The introduction of a T_d during electrochemical etching has been examined. This delay can be described as the duration during which samples experience electroless chemical etching prior to electrochemical anodisation, which is applied before connecting the power supply. However, the study solely examined porous silicon (P-Si) structures [20]. Therefore, this present study examines the effect of applying a Td in the etching process of GaN to form uniform porous GaN using both electroless and electrochemical etching methods. By investigating the impact of Td etching time, this present study aims to optimise the formation of porous GaN structures with uniform porosity and improve its optical properties. The ultimate goal is to explore the potential of these uniform porous GaN structures for enhanced P-GaN optoelectronic devices, such as LEDs and photodetectors. To the best of our knowledge, no previous study has examined applying a Td prior to pulse electrochemical etching to control the formation of P-GaN.

2. EXPERIMENTAL PROCEDURE

This present study used a 2-inch-diameter GaN wafer, unintentionally doped n-type GaN grown on a C-plane sapphire substrate, with a thickness of about 5 µm and a carrier concentration of $\sim 1x10^{18}$ cm^{-3}. The P-GaN samples were fabricated using UV-assisted DCPEC and the iPEC etching. Prior to electrochemical etching, the GaN wafer was diced into smaller dimensions of approximately 1 cm by 1 cm before being fitted in a Teflon cell. Prior to the etching process, the GaN wafer was cleaned with Aqua regia solution to remove metals from the surface. To perform the etching, a Teflon cell with the metal plate was used to hold the sample as an anode while a hole was provided for the potassium hydroxide (KOH) electrolyte. The platinum was fully utilised as a cathode for the anodisation.

The GaN sample was wrapped in aluminium (Al) foil before being installed through the O-ring so that only the front surface was exposed to the electrolyte solution. The metal plate was then tightly clamped using two screws to ensure that electrolyte leakage did not occur during the etching process. The DCPEC and iPEC etching techniques were used to fabricate a porous structure on the GaN sample at a current density of 80 mA/cm^2 for 60 minutes in an electrolyte consisting of 4% KOH under 100 W UV light. The current density was set at 80 mA/cm^2 according to the recommendations of Razali *et al.* [21]. An additional pulse cycle of 14 ms with T_{on} of 10 ms and T_{off} of 4 ms was applied on the iPEC porous sample while an additional 120 minutes were applied on the T_d P-GaN. After the etching process, all the samples were rinsed with deionised (DI) water. The KOH solution was used as an electrolyte as it interacts highly with GaN [8]. Similarly, all the samples were rinsed with deionised (DI) water post etching. Figures 1 and 2 depict the experimental setups of the DCPEC and iPEC processes, respectively. The P-GaN samples created via DCPEC were referred to as DPEC, the P-GaN samples etched via iPEC with no T^d were referred to as iPEC, and the P-GaN anodised via iPEC with T_d were referred to as T_d iPEC. An as-grown GaN samples were also included for comparison.

The surface morphology and topography of the P-GaN were characterised using a JEOL® JSM 7401F FESEM and a Bruker® Dimension® Edge™ atomic force microscopy (AFM). NanoScope Analysis was used to analyse the surface roughness and the estimated pore depth of the samples with a scan area of 5 x 5 $µm^2$. Both P-GaN samples underwent energy-dispersive X-ray spectroscopy (EDX) to determine the composition of every material present on their surface while a PANalytical® X'pert Pro MRD HR

XRD was used to assess the crystalline quality of the samples.

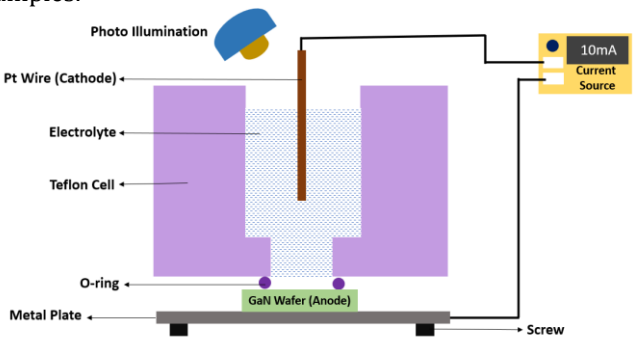

Figure 1 The experimental setup of the DCPEC etching technique.

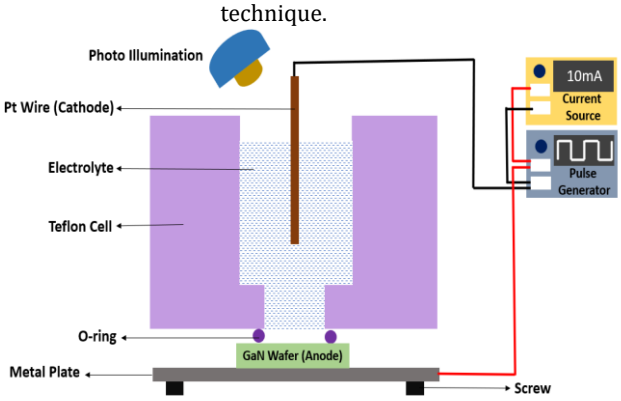

Figure 2 The experimental setup of the iPEC and T_d iPEC etching techniques.

An inVia™ Qontor Raman microscope was used to study the optical characteristics of the samples while an Edinburgh Instruments Ltd. FLS920 fluorescence spectrometer was used to examine their PL characteristics. A helium–neon (He-Ne) laser (λ=633 nm) and a Xenon (Xe) lamp (λ=325 nm) were used as excitation sources for the Raman and PL spectroscopy, respectively.

3. RESULTS AND DISCUSSIONS

Figures 3(a) to (d) depict the top-view FESEM images of the as-grown GaN and the P-GaN samples created using DCPEC, iPEC, and T_d iPEC, respectively.

As seen, the as-grown GaN sample had a smooth surface, while significant morphological differences were observed between the P-GaN samples created using the different etching techniques. More specifically, the iPEC sample exhibited a hexagonal porous structure consistent with the wurtzite structure of GaN. The morphology showed that the T_{on} and T_{off} pulse currents did not fully etch and form the porous structure, with two porous layers indicated by pores at the whiter regions and clearer hexagonal structures at the darker regions. As a result, the pulsed current etching selectively dissociated the GaN material on the surface of the anode while preserving the underlying GaN structure.

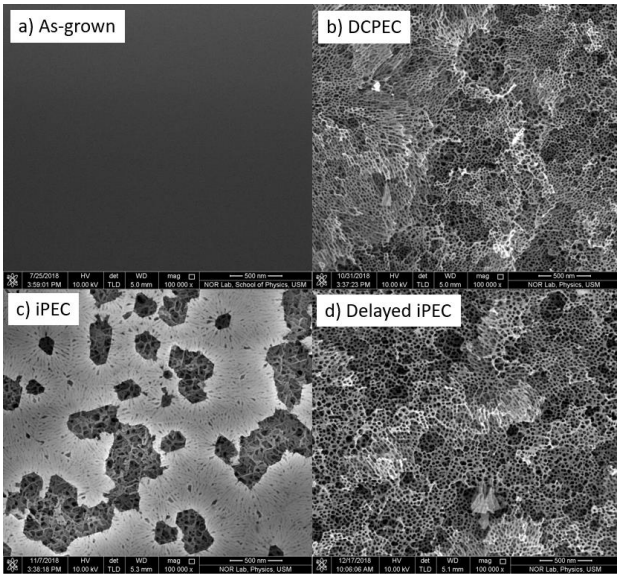

Figure 3 The top-view images of the a) as-grown GaN, b) DCPEC, c) iPEC, and d) T_d iPEC P-GaN samples.

Table 1 The average pore diameter and porosity of the P-GaN samples etched using different techniques.

Etching Technique	Average Pore Diameter (nm)	Porosity (%)
As-grown	-	-
DCPEC	256	78
iPEC	60	42
T_d iPEC	29	80

The dissolved GaN created pores, or voids, within the material to form a porous GaN structure.. Meanwhile, the T_d iPEC sample had a spongy hexagon-like structure with a smaller pore diameter, higher porosity, and a more uniform porous structure. Therefore, the T_d helped form shallower pores at some grain boundaries initially and eventually deeper pores when the pulse current was supplied. Similar spongy-pore structures have been observed on the surface of GaN etched using various techniques [20–24]. It is noteworthy that Wahab *et al.* [25] also indicated superior porosity when there is a T_d in developing porous formations on Si surfaces. Table 1 presents the average pore diameters and porosities of the P-GaN samples etched using DCPEC, iPEC, and Td iPEC. As demonstrated, Td iPEC had the smallest pore diameter of 29 nm and the highest porosity of 80%.

Figure 4 depicts the EDX spectroscopy results of the as-grown GaN and P-GaN samples. It was confirmed that only nitrogen (N), gallium (Ga), and oxygen (O) were present in significant quantities in the P-GaN samples with no trace of other elements. Table 2 summarises the elemental contents of the P-GaN samples etched using different techniques. It is evident that there was no trace of O in the iPEC sample, suggesting no surface contamination and the absence of the oxide phase post etching.

Figure 5 portrays the surface roughness and the horizontal cross-section (AFM analysis) of the as-grown and all P-GaN samples. As seen, the surface roughness of the T_d iPEC sample was higher than that of the DCPEC and iPEC samples, therefore, it had more pronounced pores. Its estimated average pore depth was also deeper than that of the DCPEC and iPEC samples.

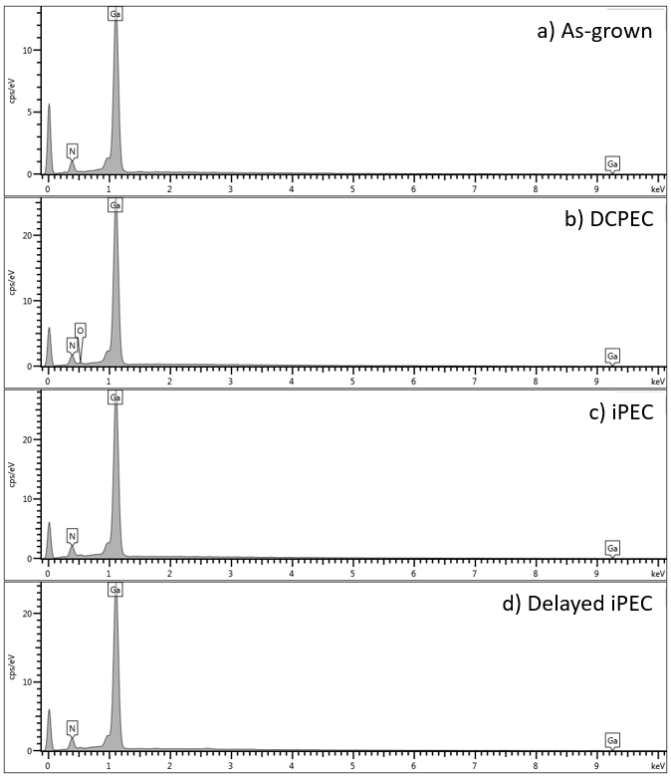

Figure 4 The EDX analysis results of the a) as-grown GaN, b) DCPEC, c) iPEC, and d) T_d iPEC P-GaN samples etched using different techniques.

Table 2 The EDX analysis results of the as-grown GaN and the P-GaN samples etched using different techniques.

Etching Technique	N At (%)	Ga At (%)	O At (%)
As-grown	31.0	69.0	-
DCPEC	38.9	58.1	3.0
iPEC	43.4	56.6	-
T_d iPEC	44.0	56.0	-

Based on the results of both the FESEM and AFM analyses, it can be concluded that the T_d iPEC sample formed uniform, smaller, and deeper pores at a higher density and a rougher surface. The variations in their etching mechanisms may explain the significant differences in pores formed in the P-GaN samples. Figure 6 provides a schematic illustration of the P-GaN pores formed by the different etching techniques.

In the DCPEC technique, the current flow was supplied without any interruptions for 60 minutes. This facilitated more gradual interactions between the electrolyte and the sample, resulting in larger but shallower pores. In the iPEC technique, however, the current flow was interrupted during T_{off}. On the next T_{on}, the electrolyte-GaN interaction tended to create new pores on the surface of the sample rather than continuing with the previously formed pores [26]. This explains why the iPEC sample produced two layers of porous structures.

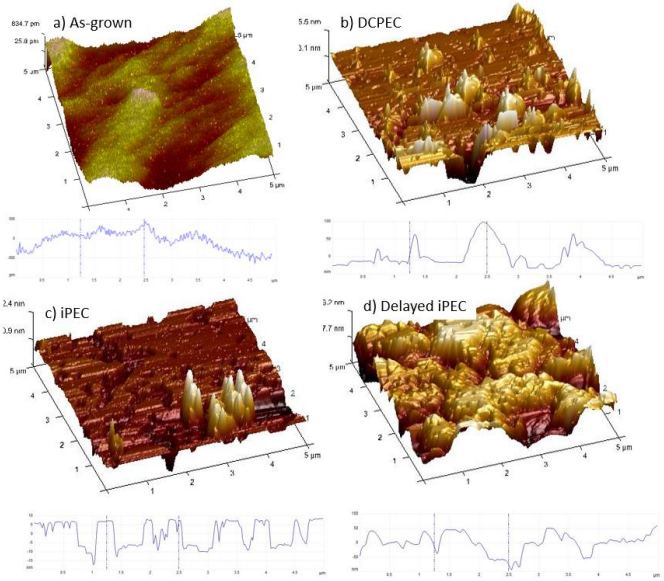

Figure 5 The AFM analysis results of the as-grown GaN and the P-GaN samples etched using different techniques.

On the other hand, during the Td, some regions of the GaN surface randomly change into oxidation or reduction sites, which involve chemical reactions with the GaN surfaces.As random points were resolved, the initial holes in the crystalline silicon became localised. As the etching conditions were uniform throughout the entire GaN surface, the homogeneous pores were created via random localisation. Meanwhile, during electrochemical etching, the flow of electrons was not uniform over the entire surface, which caused non-uniform sub-micrometer pores to form. Therefore, T_d can be considered an electroless chemical etching technique that creates shallow and uniform holes on a GaN surface and that can be used to extend pores and creater deeper and uniform pores during electrochemical etching [20,25]. Table 3 displays the average pore depths and roughness of the P-GaN sampled under various etching conditions.

Figure 7 presents the XRD analysis results of the as-grown GaN and all the P-GaN samples etched using DCPEC, iPEC, and T_d iPEC at a 2θ range from 30 to 80°. The identification of the diffraction peaks in all the samples indexed the hexagonal wurtzite GaN as JCPDS card no. 898624 with a preferred orientation towards a dominant peak (0002) at 34.53°. More specifically, the presence of a prominent sapphire (0001) peak at approximately 41.6° from the sapphire substrate was evident in the as-grown GaN. Additionally, characteristic peaks of (0001)-oriented Wurtzite GaN were observed at around 34.53 and 72.9°, which were attributed to the (0002) and (0004) diffractions of Wurtzite GaN, respectively.

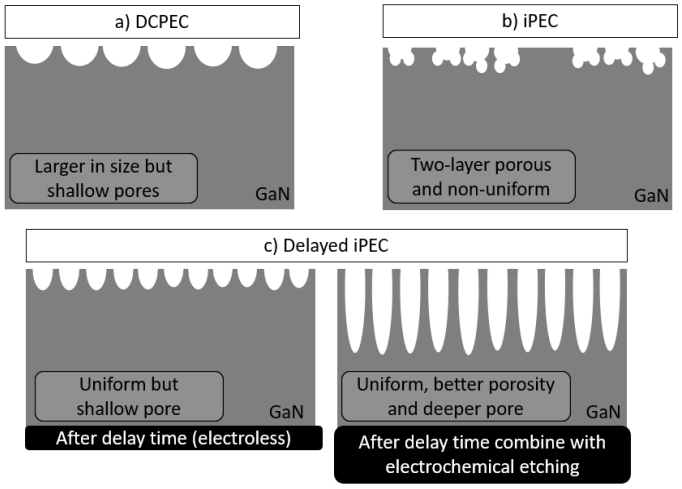

Figure 6 An illustration of the pore formed on the GaN surface using a) DCPEC, b) iPEC, and c) T_d iPEC etching techniques.

Table 3 The surface roughness and average pore depths of the as-grown GaN and the P-GaN samples etched using different techniques.

Etching Technique	Roughness in RMS value (nm)	Average Pore Depth (nm)
As-grown	0.22	-
DCPEC	32.2	32.9
iPEC	13.0	8.6
T_d iPEC	85.9	66.8

The presence of a sharply defined (0002) diffraction peak, characterised by an extremely narrow 0.15 full width at half maximum (FWHM), and the emergence of a high-order GaN (0004) diffraction peak were strong evidence of the excellent quality of the GaN film grown on a sapphire substrate. Significant differences were also observed in terms of intensity within the porous samples. The T_d iPEC sample exhibited better 2Theta-scan intensity. However, the dominant peak positions in the DCPEC, iPEC, and T_d iPEC samples were the same at 34.53°, representing a GaN (0002) diffraction. A similar peak position has also been observed in P-GaN samples [21].

The Td iPEC sample had a lower FWHM than the iPEC samples.However, the intensity of the as-grown GaN sample was higher than that of the P-GaN samples, as the etching process may have created a large number of crystal defects, which decreases crystalline quality [27]. A lower FWHM indicates better crystallinity [28]. The P-GaN samples retained the excellent quality of the as-grown sample. As recommended by Wahab *et al.* [25], the Debye-Scherer equation was used to calculate the crystallite sizes of the samples. A difference was observed between the iPEC and T_d iPEC samples. On the other hand, the sizes of the crystallites in T_d iPEC sample were larger as its FWHM was smaller. Table 4 summarises the 2Theta-scan analysis results of the P-GaN samples etched using different techniques.

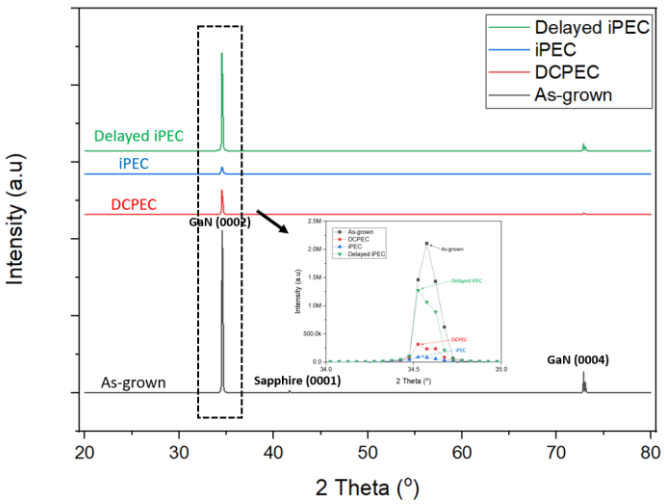

Figure 7: The XRD patterns of the as-grown GaN and the P-GaN samples etched using different techniques. The inset is an enlarged image of the GaN (0002) diffraction peak.

Table 4 The 2Theta-scan results of the as-grown GaN and the P-GaN samples etched using different techniques.

Etching Technique	Peak Position (°)	Peak Intensity (a.u)	FWHM	Crystallite Size (nm)
As-grown	34.58	2.11 M	0.15	579.10
DCPEC	34.53	317.41 K	0.17	510.92
iPEC	34.53	90.23 K	0.20	434.28
T_d iPEC	34.53	1.27 M	0.16	542.86

Figure 8 depicts the Raman spectroscopy results for all of the as-grown GaN and the P-GaN samples. All the P-GaN samples exhibited allowable phonon mode of E_2 (high) at 569.01 cm^{-1} and a relatively small peak of A_1 (TO) forbidden modes at 561.6 cm^{-1}. The Raman spectra showed a peak shift to a higher frequency than the as-grown sample (567.96 cm^{-1}). The E_2 (high) phonon's position was due to GaN stress. As a result, it was a useful indicator for assessing the GaN strain condition. In all the porous GaN samples, the E_2 (high) peak shifted towards higher frequencies than the as-grown GaN sample (567.96 cm^{-1}). The relaxation of the residual stress can be quantified using Equation 1 [29]:

$$\sigma = \Delta\omega/4.3 \ (cm^{-1}\ GPa^{-1}) \quad (1)$$

where, σ is the biaxial stress and $\Delta\omega$ is the E_2(high) phonon peak shift. This 569.01 cm^{-1} shift corresponds to a 0.24 GPa tensile stress relaxation in the P-GaN sample [29]. As no broadening of the Raman peak was observed, it indicated minimal structural disorder. Li *et al.* [23] and Razali *et al.* [26] also observed identical peak positions. Because no broadening had occurred, the FWHM was similar in all porous samples. The Raman spectra intensity of T_d iPEC sample was slightly higher than that of the DCPEC and the iPEC samples. This indicates that the

porous structure of the T_d iPEC sample scatters light more efficiently [23]. Table 5 summarises the Raman analysis results of the P-GaN etched using different techniques.

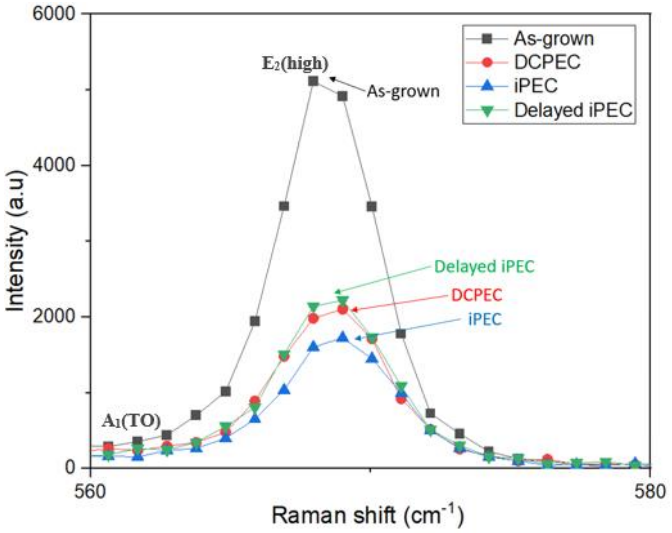

Figure 8 The Raman analysis results of the as-grown GaN and the P-GaN samples etched using different techniques.

Table 5 The Raman analysis results of the as-grown GaN and the P-GaN samples etched using different techniques.

Etching Technique	Peak Position (°)	Peak Intensity (a.u)	FWHM	Relative Intensity
As-grown	567.96	5115.0	6.27	0
DCPEC	569.01	2105.0	6.27	-0.65
iPEC	569.01	1726.6	6.27	-0.73
T_d iPEC	569.01	2223.1	6.27	-0.65

Figure 9 displays the PL spectroscopy analysis results of the as-grown GaN and all the P-GaN samples at the 0 to 400 nm wavelength range. A slight difference in the peak position of the P-GaN sample was observed, indicating that porosity minimally affected the PL peak shift. The iPEC and the T_d iPEC samples had a peak wavelength of 363 nm that shifted to a lower wavelength, corresponding to the as-grown (364 nm).

On the other hand, the PL peak intensity of the T_d iPEC sample was higher than that of the DCPEC and iPEC samples, indicating that porosity greatly impacts the PL peak intensities. The intensity of the emitted light was proportional to the number of photons emitted [12], indicating that the Td iPEC sample emitted significantly more photons. This was due to the higher porosity of T_d iPEC sample and the significantly higher exposure of its GaN molecules to PL excitation lights, which enabled a high number of its electrons to participate in the excitation and recombination process. Table 6 summarises the PL analysis results of the P-GaN samples etched using different techniques.

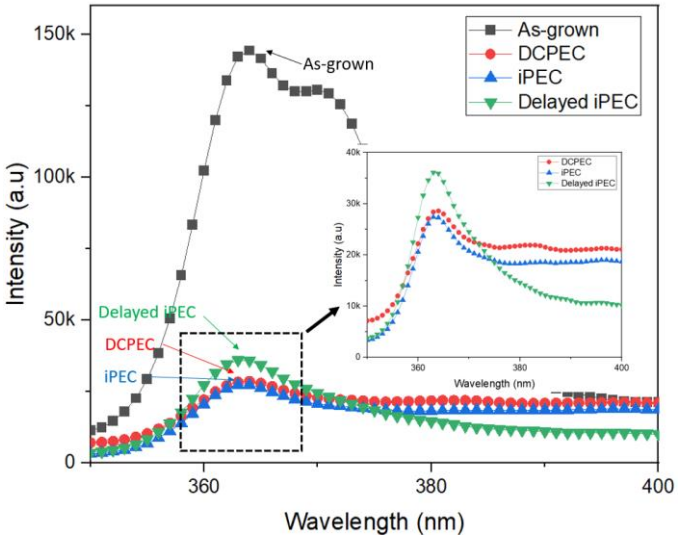

Figure 9 The PL analysis results of the as-grown GaN and the P-GaN samples etched using different techniques.

Table 6 The PL analysis results of the as-grown GaN and the P-GaN samples etched using different techniques.

Etching Technique	Peak Wavelength (nm)	Peak Intensity (a.u)	Calculated Eg (V)
As-grown	364	144.36 K	3.41
DCPEC	364	28.63 K	3.41
iPEC	363	27.35 K	3.42
T_d iPEC	363	36.11 K	3.42

4. CONCLUSIONS

Three different etching techniques; namely, DCPEC, iPEC, and T_d iPEC; were used to successfully fabricate P-GaN. The differences between the porous samples were caused by variations in the etching mechanisms.The FESEM results indicated distinct differences when using different etching techniques and introducing a T_d in the etching process. The DCPEC etching technique generated larger but shallower pores, while those of the iPEC etching technique created two layers of non-uniform pore structures. However, the introduction of a T_d significantly enhanced the physical characteristics of the iPEC sample, including its porosity, surface roughness, and pore depth. The results of the XRD analysis revealed that the T_d iPEC sample had better 2Theta-scan intensity. Its FWHM was also lower than that of the iPEC and DCPEC samples, indicating better crystalline quality. A slight peak shift was observed in the Raman analysis, corresponding to the as-grown GaN, which suggests that pore size has a minimal effect on stress relaxation. However, the PL peak intensity of the T_d iPEC sample was higher than that of the other porous samples, indicating that a greater number of electrons participated in the excitation and recombination processes, which, potentially enhanced the performance of the optoelectronic device.

ACKNOWLEDGMENTS

This project was funded by the Universiti Teknologi MARA through the Geran Penyelidikan MyRA (600-RMC/GPM ST 5/3 (023/2021)). The authors would like to thank Universiti Teknologi MARA, Cawangan Pulau Pinang and the staff of Nano-optoelectronics Research and Technology (NOR) laboratory of Universiti Sains Malaysia for supporting this research.

REFERENCES

[1] H. Lu, M. Jin, Z. Zhang, S. Wu, and L. Shui, "Wafer-Scale Fabrication and Transfer of Porous Silicon Films as Flexible Nanomaterials for Sensing Application," *Nanomaterials*, vol. 12, no. 7, 2022, doi: 10.3390/nano12071191.

[2] N. Badi, A. M. Theodore, A. Roy, S. A. Alghamdi, A. O. M. Alzahrani, and A. Ignatiev, "Preparation and Characterization of 3D Porous Silicon Anode Material for Lithium-Ion Battery Application," *Int. J. Electrochem. Sci.*, vol. 17, pp. 1–12, 2022, doi: 10.20964/2022.06.29.

[3] T. S. T. Amran, M. R. Hashim, N. K. Ali, H. Yazid, and R. Adnan, "The role of pulse time Toff on porous silicon as template for Au nanoparticles by using the integrated electrochemical technique," *Phys. B Condens. Matter*, vol. 407, no. 23, pp. 4540–4544, 2012, doi: 10.1016/j.physb.2012.08.008.

[4] G. Y. Ayvazyan, "Electrical Characteristics of Nanostructured Porous Silicon," *Inf. Technol. Electron. Radio Eng.*, pp. 87–95, 2021, doi: 10.53297/18293336-2021.2-88.

[5] S. F. Cheah, S. C. Lee, S. S. Ng, F. K. Yam, H. Abu Hassan, and Z. Hassan, "Luminescence evolution of porous GaN thin films prepared via UV-assisted electrochemical etching," *J. Lumin.*, vol. 159, pp. 303–311, 2015, doi: 10.1016/j.jlumin.2014.11.028.

[6] J. K. Liou, C. C. Chen, P. C. Chou, Z. J. Tsai, Y. C. Chang, and W. C. Liu, "Implementation of a high-performance GaN-based light-emitting diode grown on a nanocomb-shaped patterned sapphire substrate," *IEEE J. Quantum Electron.*, vol. 50, no. 12, pp. 973–980, 2014, doi: 10.1109/JQE.2014.2365022.

[7] A. Mahmood, Z. Hassan, Yam Fong Kwong, Chuah Lee Siang, and M. B. Md Yunus, "Photoluminescence, Raman and X-ray diffraction studies of porous GaN grown on sapphire," *2011 IEEE Colloq. Humanit. Sci. Eng. CHUSER 2011*, pp. 677–681, 2011, doi: 10.1109/CHUSER.2011.6163819.

[8] K. Al-Heuseen, M. R. Hashim, and N. K. Ali, "Effect of different electrolytes on porous GaN using photo-electrochemical etching," *Appl. Surf. Sci.*, vol. 257, no. 14, pp. 6197–6201, 2011, doi: 10.1016/j.apsusc.2011.02.031.

[9] F. K. Yam and Z. Hassan, "Structural and optical characteristics of porous GaN generated by electroless chemical etching," *Mater. Lett.*, vol. 63, no. 8, pp. 724–727, 2009, doi: 10.1016/j.matlet.2008.12.040.

[10] Y. Kumazaki, Z. Yatabe, and T. Sato, "Formation of GaN porous structures with improved structural controllability by photoassisted electrochemical etching," *Jpn. J. Appl. Phys.*, vol. 55, no. 4, 2016, doi: 10.7567/JJAP.55.04EJ12.

[11] F. K. Yam, Z. Hassan, and S. S. Ng, "Porous GaN prepared by UV assisted electrochemical etching," *Thin Solid Films*, vol. 515, no. 7–8, pp. 3469–3474, 2007, doi: 10.1016/j.tsf.2006.10.104.

[12] M. R. Zhang, S. J. Qin, H. D. Peng, and G. B. Pan, "Porous GaN photoelectrode fabricated by photo-assisted electrochemical etching using ionic liquid as etchant," *Mater. Lett.*, vol. 182, pp. 363–366, 2016, doi: 10.1016/j.matlet.2016.07.024.

[13] K. Al-Heuseen and M. K. Alquran, "Stress relaxation in porous GaN prepared by UV assisted electrochemical etching," *IOP Conf. Ser. Mater. Sci. Eng.*, vol. 305, no. 012015, 2018, doi: 10.1088/1757-899X/305/1/012015.

[14] A. Mahmood *et al.*, "Structural and optical studies of undoped porous GaN prepared by Pt-assisted electroless etching," *Mater. Sci. Forum*, vol. 846, pp. 358–365, 2016, doi: 10.4028/www.scientific.net/MSF.846.358.

[15] L. S. Chuah, Z. Hassan, C. W. Chin, and H. A. Hassan, "Surface morphology and formation of nanostructured porous GaN by UV-assisted electrochemical etching," *World Acad. Sci. Eng. Technol.*, vol. 55, pp. 16–19, 2009.

[16] A. F. Abd Rahim, M. S. Abdullah, A. Mahmood, N. K. Ali, and M. Mohamed Zahidi, "Quantum confinement of integrated pulse electrochemical etching of porous silicon for metal semiconductor metal photodetector," *Mater. Sci. Forum*, vol. 846, pp. 245–255, 2016, doi: 10.4028/www.scientific.net/MSF.846.245.

[17] M. R. Beghoul, N. Boutaoui, H. Bouridah, R. Remmouche, M. H. Arada, and H. Haoues, "Experimental study of n-type porous silicon obtained under illumination," *Optik (Stuttg).*, pp. 161–165, 2018, doi: 10.1016/j.ijleo.2018.01.118.

[18] M. Kadlecikova *et al.*, "Raman spectroscopy of porous silicon substrates," *Optik (Stuttg).*, vol. 174, pp. 347–353, 2018, doi: 10.1016/j.ijleo.2018.08.084.

[19] M. Kopani *et al.*, "Effect of etching time on structure of p-type porous silicon," *Appl. Surf. Sci.*, pp. 1–4, 2018, doi: 10.1016/j.apsusc.2018.04.228.

[20] N. Naderi and M. R. Hashim, "A combination of electroless and electrochemical etching methods for enhancing the uniformity of porous silicon substrate for light detection application," *Appl. Surf. Sci.*, vol. 258, no. 17, pp. 6436–6440, 2012, doi: 10.1016/j.apsusc.2012.03.056.

[21] N. S. M. Razali, A. F. A. Rahim, R. Radzali, A. Mahmood, and M. F. B. Anuar, "Morphological, structural and optical characteristics of porous GaN fabricated by UV-assisted electrochemical etching," *Solid State Phenom.*, vol. 301 SSP, pp. 3–

11, 2020, doi: 10.4028/www.scientific.net/SSP.301.3.

[22] N. M. Ahmed *et al.*, "Nano and micro porous GaN characterization using image processing method," *Optik (Stuttg).*, vol. 123, no. 12, pp. 1074–1078, 2012, doi: 10.1016/j.ijleo.2011.07.034.

[23] Q. Li *et al.*, "A perovskite/porous GaN crystal hybrid structure for ultrahigh sensitivity ultraviolet photodetectors," *J. Mater. Chem. C*, vol. 10, no. 21, pp. 8321–8328, 2022, doi: 10.1039/d2tc01207c.

[24] L. Liu *et al.*, "Nucleation mechanism of GaN crystal growth on porous GaN/sapphire substrates," *CrystEngComm*, vol. 24, no. 10, pp. 1840–1848, 2022, doi: 10.1039/d2ce00017b.

[25] N. H. A. Wahab, A. F. A. Rahim, A. Mahmood, R. Radzali, and Y. Yusof, "Investigation on the effect of delay time during pulse chemical etching of porous silicon formation," *Acta Phys. Pol. A*, vol. 135, no. 5, pp. 873–876, 2019, doi: 10.12693/APhysPolA.135.873.

[26] N. S. M. Razali *et al.*, "Investigation on the effect of direct current and integrated pulsed electrochemical etching of N-type (100) silicon," *Acta Phys. Pol. A*, vol. 135, no. 4, pp. 697–701, 2019, doi: 10.12693/APhysPolA.135.697.

[27] X. Zhai, Y. Zhang, Y. Zhang, M. Zhang, and J. Tang, "Facile fabrication of 3D honeycomb-like porous GaN photoanode for reliable and sensitive photoelectrochemical detection of glucose," *J. Alloys Compd.*, vol. 939, p. 168784, 2023, doi: 10.1016/j.jallcom.2023.168784.

[28] R. Radzali, M. Z. Zakariah, A. Mahmood, A. F. A. Rahim, Z. Hassan, and Y. Yusof, "The effect of ecthing duration on structural properties of porous Si fabricated by a new two-steps alternating current photo-assisted electrochemical etching (ACPEC) technique for MSM photodetector," *AIP Conf. Proc.*, vol. 1875, pp. 020003 (1–10), 2017, doi: 10.1063/1.4998357.

[29] J. Yu, L. Zhang, J. Shen, Z. Xiu, and S. Liu, "Wafer-scale porous GaN single crystal substrates and their application in energy storage," *CrystEngComm*, vol. 18, no. 27, pp. 5149–5154, 2016, doi: 10.1039/c6ce00741d.